Supplementary Information

Pd-coated Ru nanocrystals supported on N-doped graphene as HER and ORR electrocatalyst

Barun Kumar Barman, Bidushi Sarkar and Karuna Kar Nanda*

Materials Research Centre, Indian Institute of Science, Bangalore-560012, India.

*E-mail: nanda@iisc.ac.in, Fax: +91 80 2360 7316; Tel: +91 80 2293 2996

Experimental Details:

Reagents: Ruthenium (III) chloride hydrate (99.98% trace metals), Sodium tetrachloropalladate (II) (99.99% trace metals), melamine, Pt/C (20 weight %), Pd/C (10 weight %) and Nafion (5 wt %) were purchased from Sigma-Aldrich. A Merck Milli-Q system Millipore water was used throughout the experiment.

Synthesis of Ru@NG: Ruthenium chloride (250 mg) and melamine (1 g) were taken in a mortar pestle and ground well. It was transferred to a closed quartz tube sealed at one end and pyrolyzed in a tube furnace at 900 °C for 1 h. The as-obtained black product is collected and named Ru@NG.

Synthesis of Pd layer on Ru@NG (Pd-Ru@NG): As-synthesized Ru@NG (100 mg) was dipped in 10 mM solution of sodium tetrachloropalladate for 12 h and left undisturbed. It was then centrifuged; the product was washed properly with water-ethanol and dried at 70 °C. The as-obtained product is collected and named Pd-Ru@NG.

Synthesis of Pt layer on Ru@NG (Pt-Ru@NG): Similarly, we have synthesized Pt layer on Ru@NG by simply replacing 10 mM solution of sodium tetrachloropalladate with potassium

tetrachloroplatinate and followed the same procedure. The product was washed multiple times with water-ethanol and dried. The as-obtained product is named Pt-Ru@NG.

Characterizations:

The as-synthesized samples were characterized using X-ray diffraction (XRD), 2θ scan range of 10 to 90° using an X-ray diffractometer (PANalytical) with Cu Kα radiation, 1.54 Å at room temperature. Raman spectra of the samples were recorded on a WITec system at a 532 nm excitation wavelength using Nd: YAG laser. The scanning electron microscopy (SEM) images and energy-dispersive X-ray spectroscopy (EDS) and mapping were obtained using FESEM FEI Inspect 50. Transmission electron microscopy (TEM), high-resolution transmission electron microscopy (HRTEM), high-angle annular dark-field scanning transmission electron microscopy (HAADF-STEM) and elemental mapping characterizations were carried out using JEOL-JEM-2100F at an accelerating voltage of 200 kV. X-ray photoelectron spectroscopy (XPS) was carried out on ESCALAB 250 Thermo Scientific with a monochromatic Al Kα, 1486.6 eV source.

Electrocatalytic Measurements:

The catalyst ink was prepared by taking 2 mg of as-synthesized catalyst and adding 200 µL of ethanol and 20 µL of Nafion solution (5 wt %). The solution was sonicated for 30 min and then 3 µL drop cast onto glassy carbon rotating disc electrode working electrode (RDE; 3 mm diameter and 0.07/cm^2) and dried at 70 °C which resulted in catalyst loading of 0.38 mg/cm^2. All the electrochemical studies were carried out on a three-electrode set-up, CHI750E workstation. Pt wire and an Ag/AgCl electrode were used as counter and reference electrodes, respectively. All hydrogen evolution reaction (HER) measurements were carried

out in 1 M KOH solution and 1 M H_2SO_4 solution after purging with N_2 gas for 30 min. The potential measured against Ag/AgCl was converted to potential versus reversible hydrogen electrode (RHE) according to the equation, $E_{(vs\ RHE)} = E_{(vs\ Ag/AgCl)} + E_{Ag/AgCl}^{\circ} + 0.059*pH$. The HER measurements were also performed with graphite rod as the counter electrode.

The catalytic activity of as-synthesised catalyst was compared with commercial Pt/C (20 wt %) and Pd/C (10 wt %) having a catalyst loading of 0.38 mg/cm^2 on RDE. The oxygen reduction reaction (ORR) measurements were performed in 0.1 M KOH solution. N_2 and O_2 were purged into the solution for about 40 min to achieve an O_2 free and O_2 saturated condition, respectively. The RDE measurements were carried out at different rotation speeds (600 to 1800 rpm) in the N_2 and O_2-saturated solution. The methanol tolerance test was done by adding 1 M methanol to the solution. The Koutecky–Levich (K–L) plot between the inverse current density (J^{-1}) as a function of the inverse of the square root of the rotation speed ($\omega^{-1/2}$) at different potentials was done using following equation,

$$1/J = 1/J_k + 1/J_d$$

where J, J_k, and J_d represent the total current density, kinetic current density and diffusion current density, respectively. Levich equation was used to calculate the overall number of electrons transferred and is given by,

$$J_d = 0.62nFD_{O2}^{2/3}\ \nu^{-1/6}\ C_{O2}\ \omega^{1/2}$$

where n = overall number of electrons transferred in the process, F = 96 485 C/mol (Faraday constant), $D_{O2} = 1.9 \times 10^{-5}$ cm^2/s (bulk diffusion coefficient of oxygen in the electrolyte), ν = 0.01 cm^2/s (kinematic viscosity of the electrolyte), $C_o = 1.2 \times 10^{-6}$ mol/cm^3 (concentration of oxygen dissolved in the electrolyte), ω = angular velocity of the working electrode.

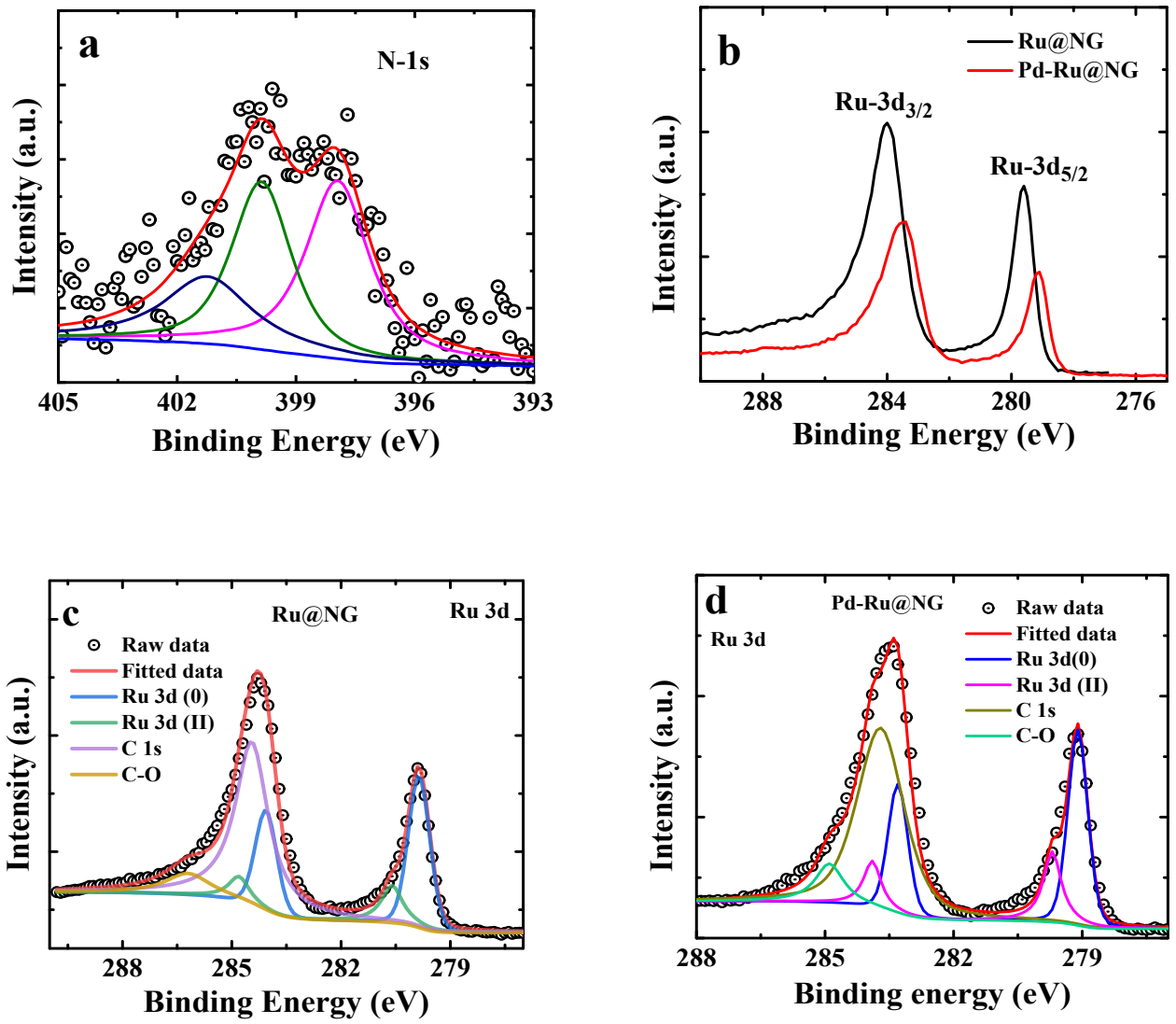

Fig. 1 Deconvoluted HRXPS spectra of (a) N-1s of Pd-Ru@NG. (b-d) Ru 3d of Ru@NG, and Pd-Ru@NG, respectively.

ESI-2

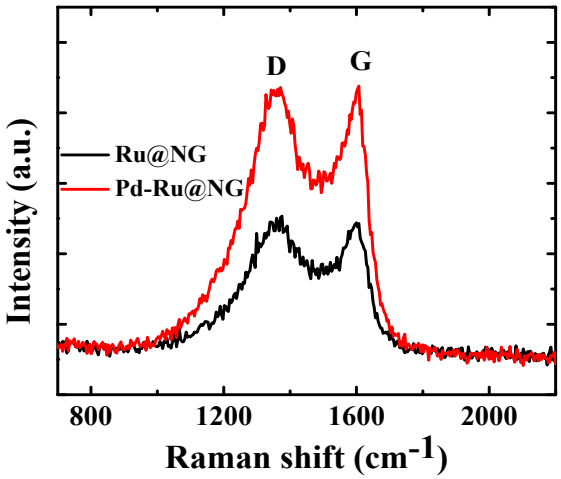

Fig. 2 Raman spectra of Ru@NG and Pd-Ru@NG hybrid, respectively.

ESI-3

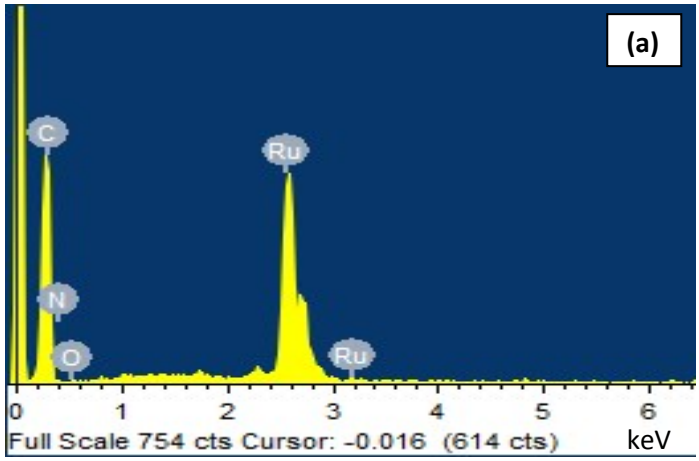

Element	Weight%	Atomic%
C K	39.80	70.99
N K	7.92	13.52
O K	3.60	4.93
Ru L	48.69	10.56
Totals	100.00	

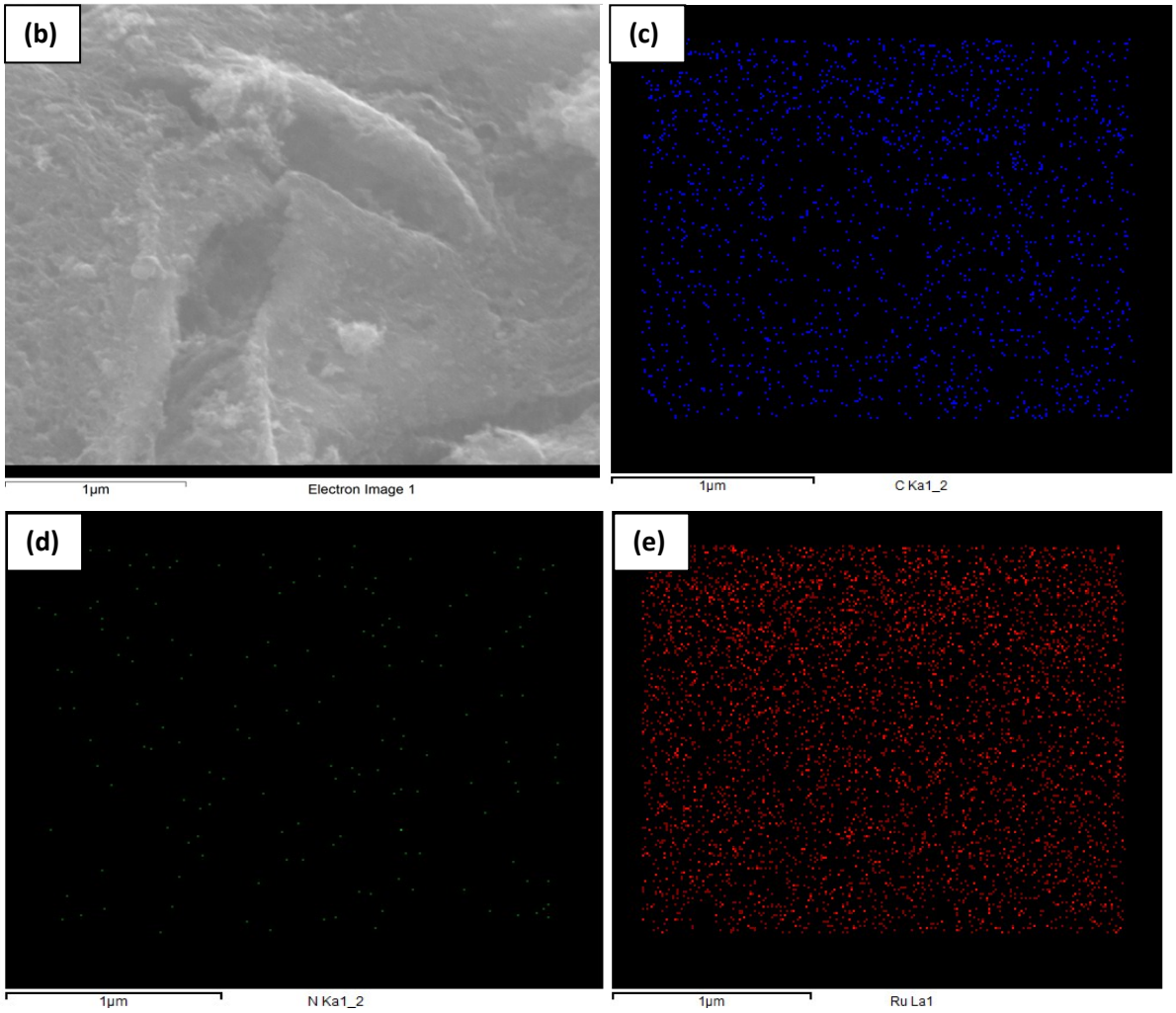

Fig. 3 (a) EDS spectra and the elemental composition table. (b) SEM image. (c-e) elemental mapping of C, N, and Ru, respectively of Ru@NG

ESI-4

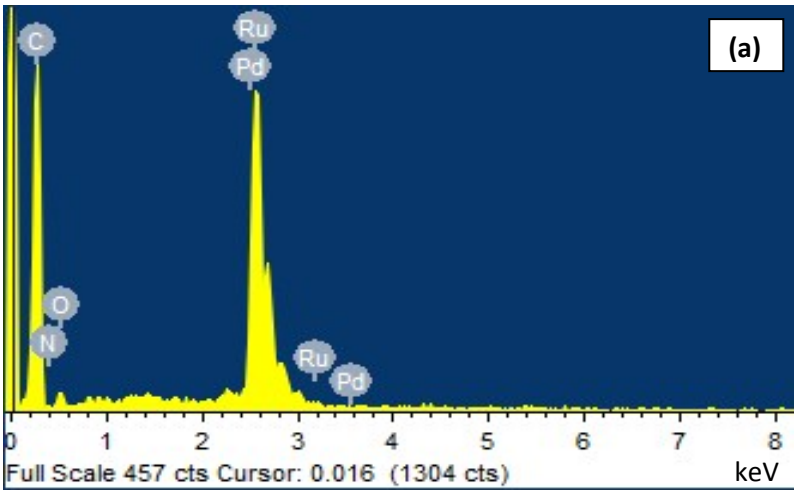

Element	Weight%	Atomic%
C K	35.67	63.34
N K	8.98	13.68
O K	10.12	13.49
Ru L	40.04	8.45
Pd L	5.19	1.04
Totals	100.00	

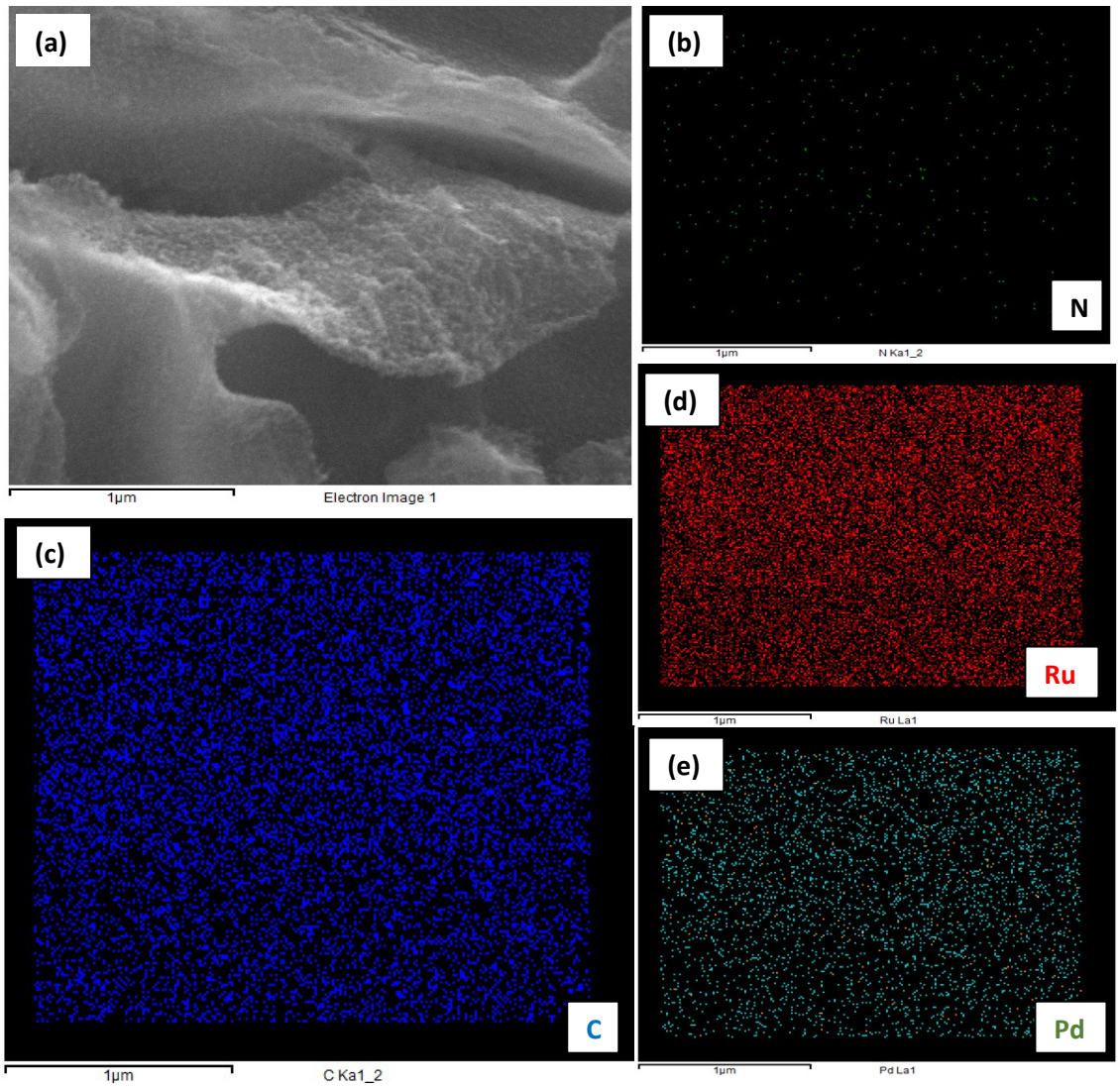

Fig. 4 (a) EDS spectra of Ru@NG and the elemental composition table. (b) SEM image. (c-e) elemental mapping of C, N, and Ru, respectively of Pd-Ru@NG

ESI-5

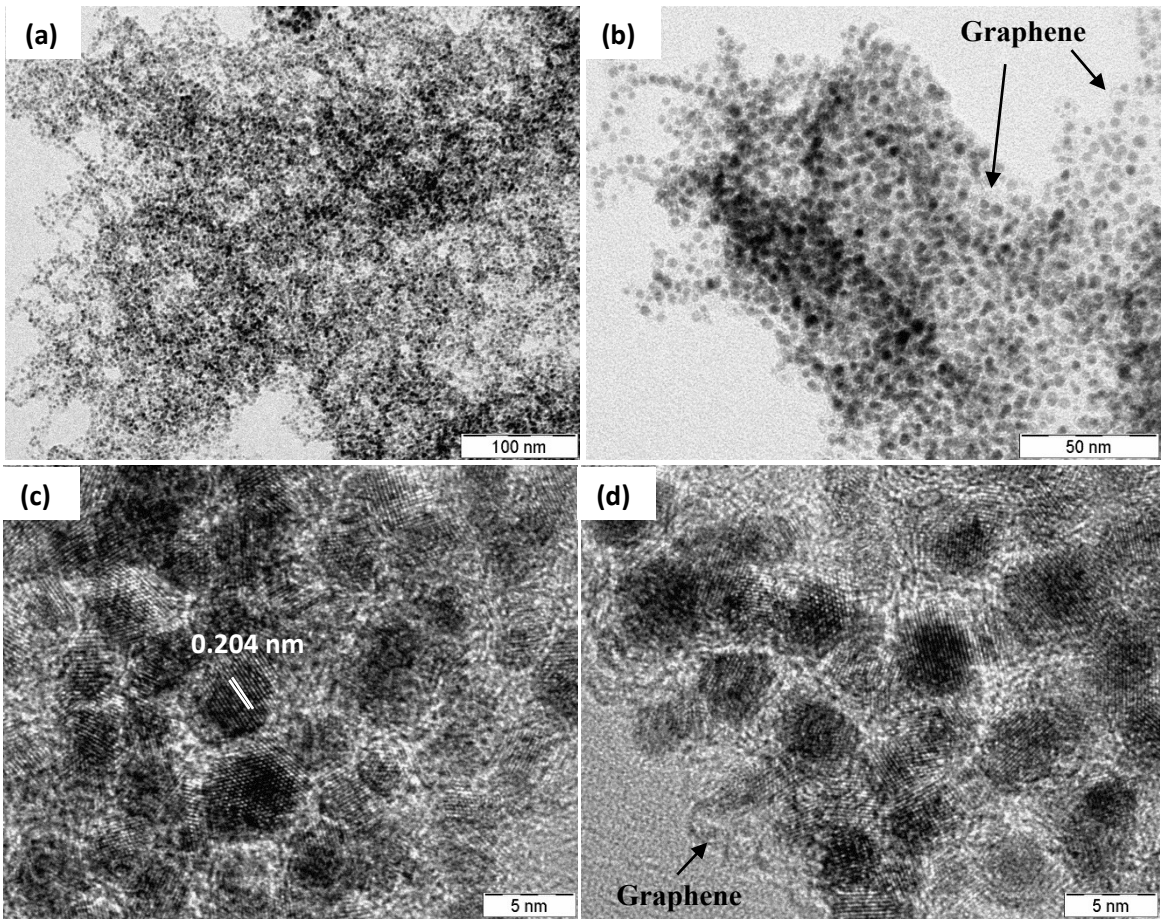

Fig. 5 (a, b) TEM. and (c, d) HRTEM image of Ru@NG

ESI-6

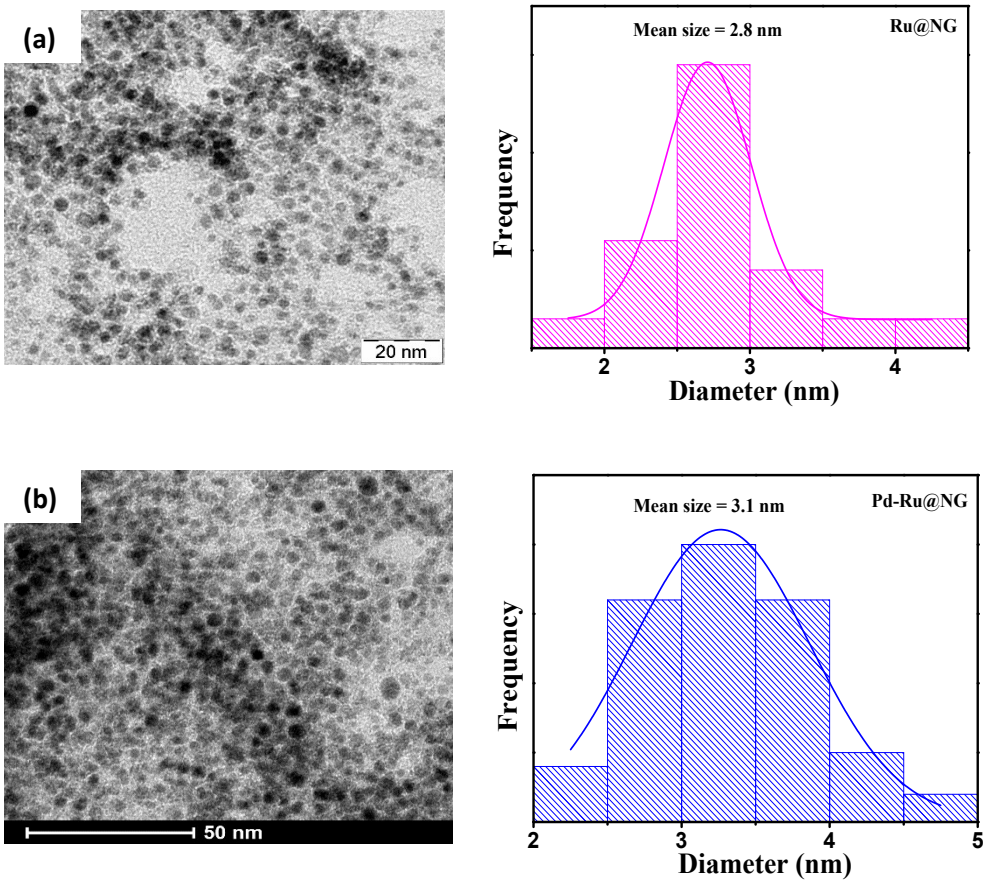

Fig. 6 TEM image and corresponding average particle size curve of (a) Ru@NG. (b) Pd-Ru@NG

ESI-7

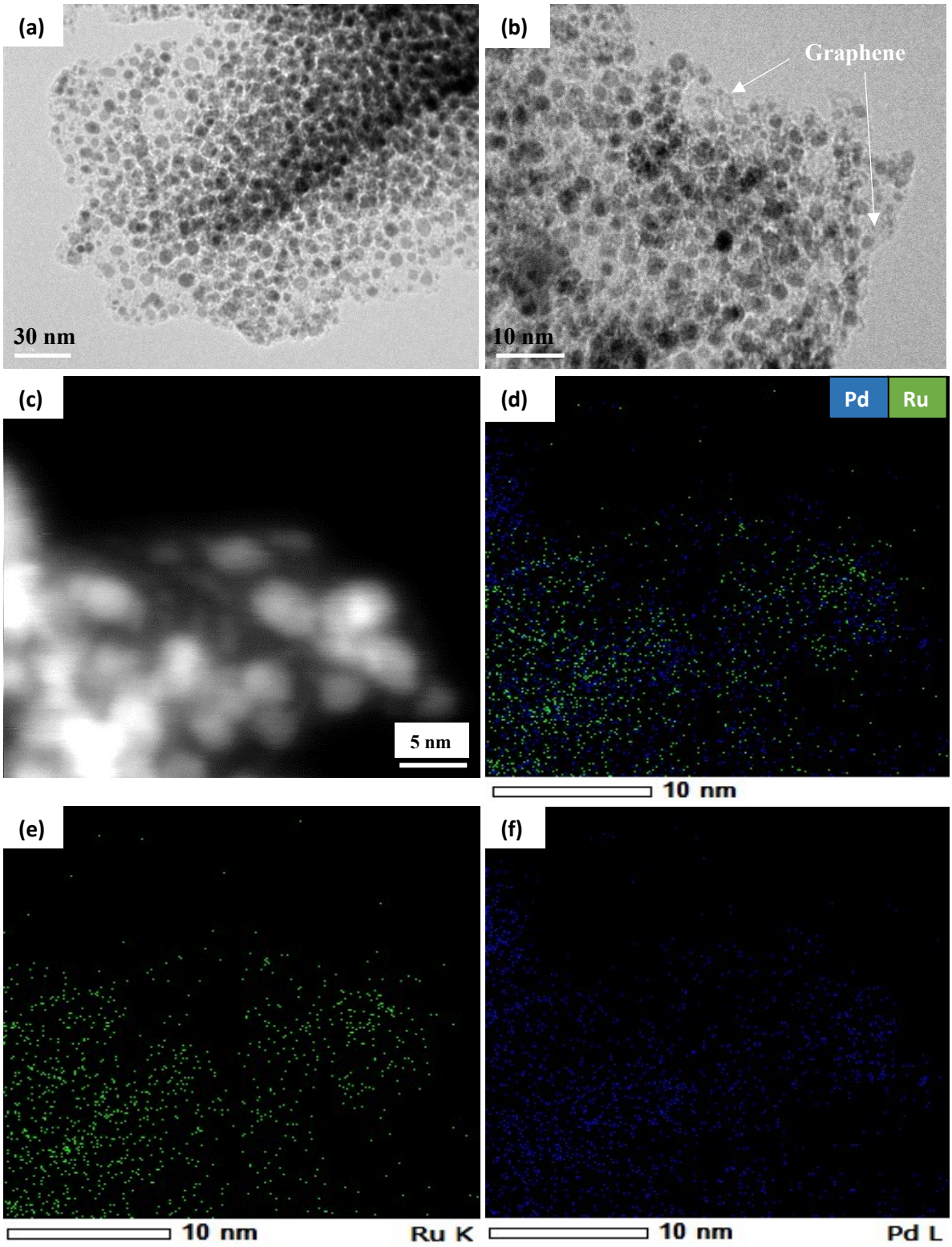

Fig. 7 (a,b) TEM image. (c) HAADF-STEM image. and (d-f) TEM elemental mapping of overlapped Pd-Ru, Ru and Pd, respectively of Pd-Ru@NG

ESI-8

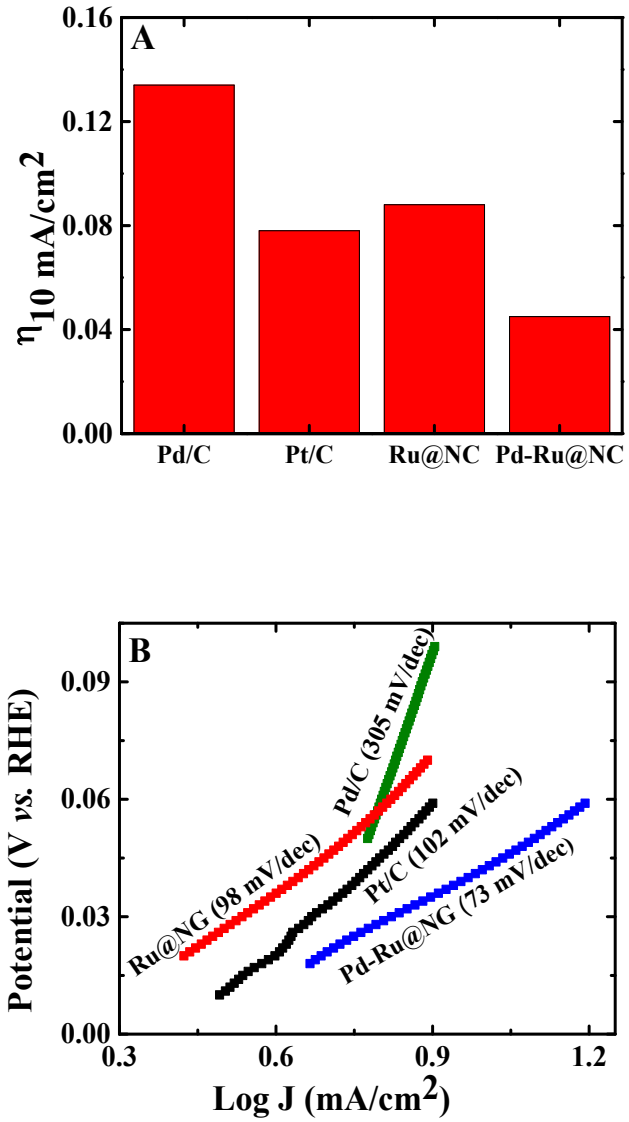

Fig. 8 (a) Comparison of HER activity of the catalysts and (b) Tafel slope of different catalyst in 1 M KOH medium

ESI-9

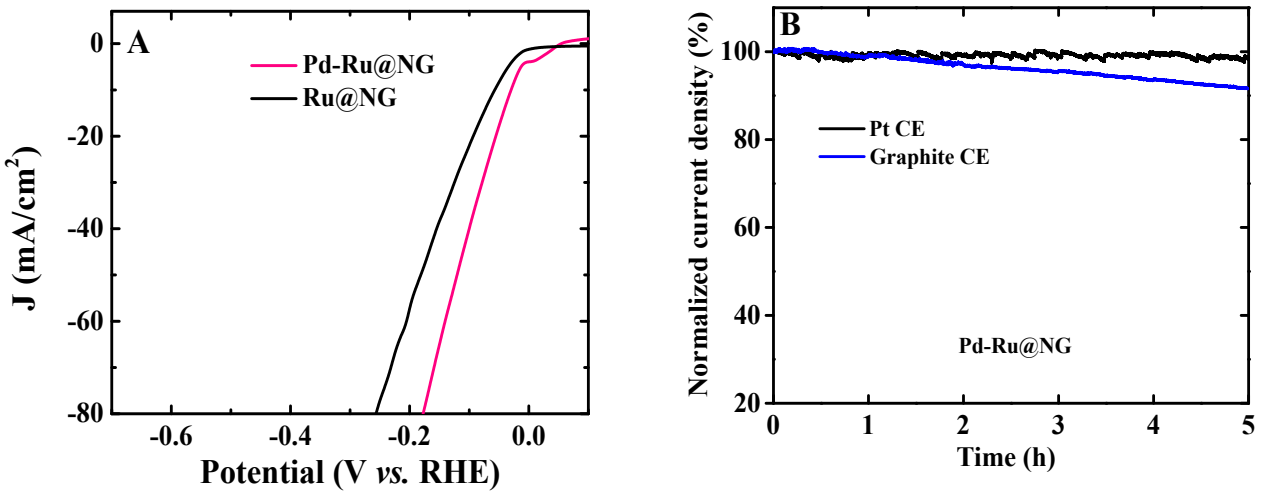

Fig. 9 (a) LSV of Pd-Ru@NG and Ru@NG with graphite rod as the counter electrode (CE), and (b) Normalized chronoamperometric stability of the Pd-Ru@NG with Pt and graphite rod as the CE in 1 M H_2SO_4 solution.

The graphite rod is used as the counter electrode to consider any Pt leaching that might interfere with the catalytic activity. With graphite rod as CE, although the current density decreases slightly, the potential required to reach a current density of 10 mA/cm^2 remains similar and the current retention is up to 92 % after 5 h. This ensures that the HER activity seen in intrinsic of the catalyst and not influenced by Pt leaching.

ESI-10

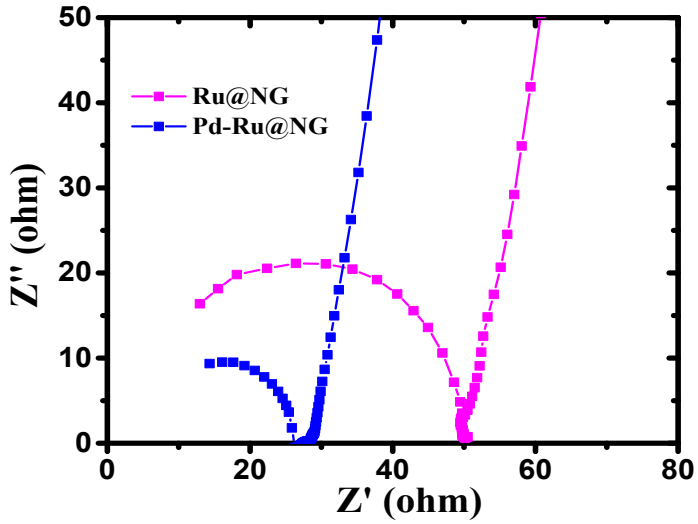

Fig. 10 Electrochemical impedance spectroscopy (EIS) measurements for Ru@NG and Pd-Ru@NG in alkaline medium, 1 M KOH at an overpotential of 20 mV.

ESI-11

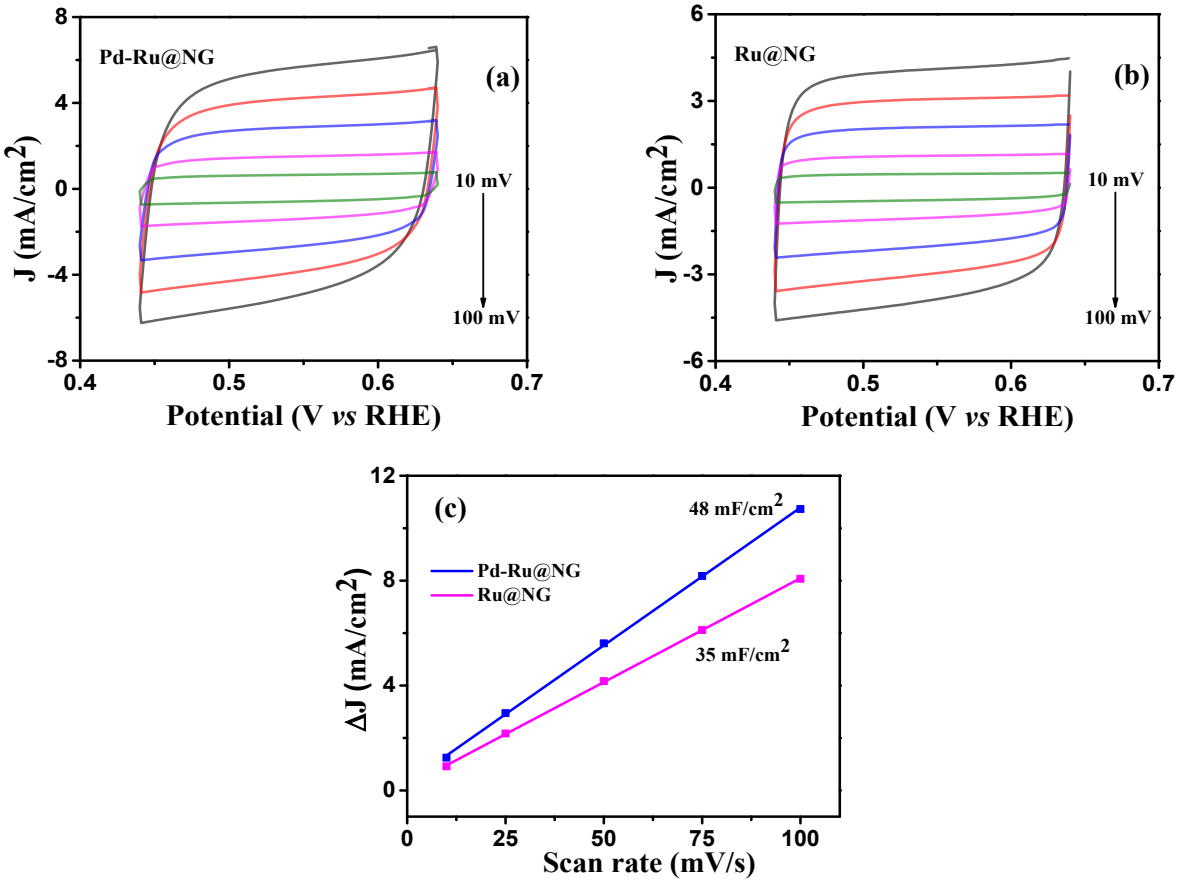

Fig. 11 (a and b) CV curves in the non-faradaic region of Pd-Ru@NG and Ru@NG at different scan rates from 10 to 100 mV/s. (c) C_{dl} plot for Pd-Ru@NG and Ru@NG

The C_{dl} has been determined by cyclic voltammetry (CV) measurements in the non-redox regime in 1 M KOH solution with different scan rates.

ESI-12

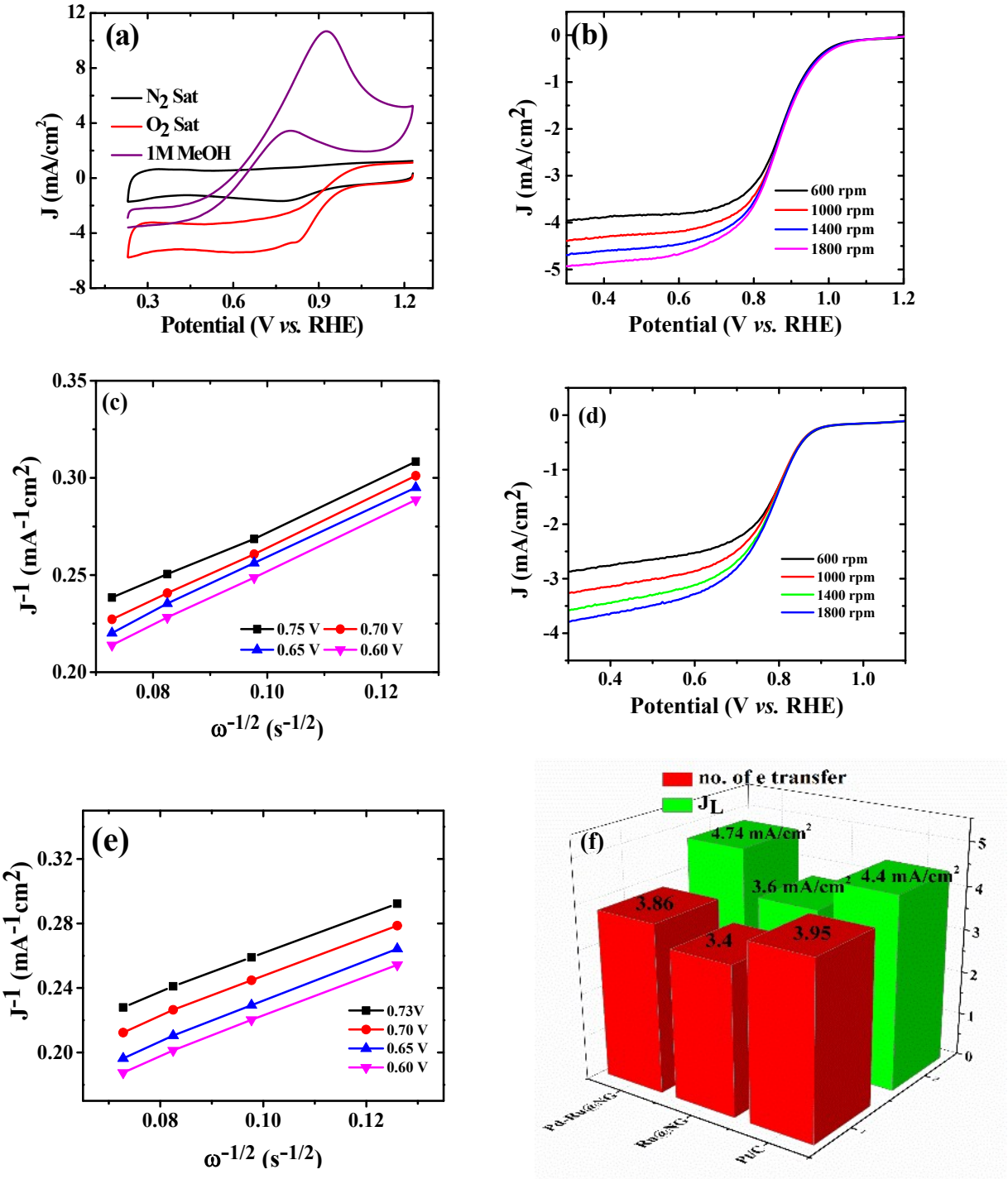

Fig. 12 (a) CV of Pt/C (20 wt%) in N_2 saturated (sat.), O_2 sat. 0.1 M KOH and 1 M methanol at a rotation speed of 600 and a scan rate of 50 mV/s. (b and c) LSV curve at different rotation speed at 10 mV/s scan rate and the corresponding K-L plot for Pt/C. (d and e) LSV polarization curve and K-L plot of Ru@NG. (f) Bar graph depicting no. of electrons transferred and the limiting current density for Pt/C, Ru@NG and Pd-Ru@NG.

ESI-13

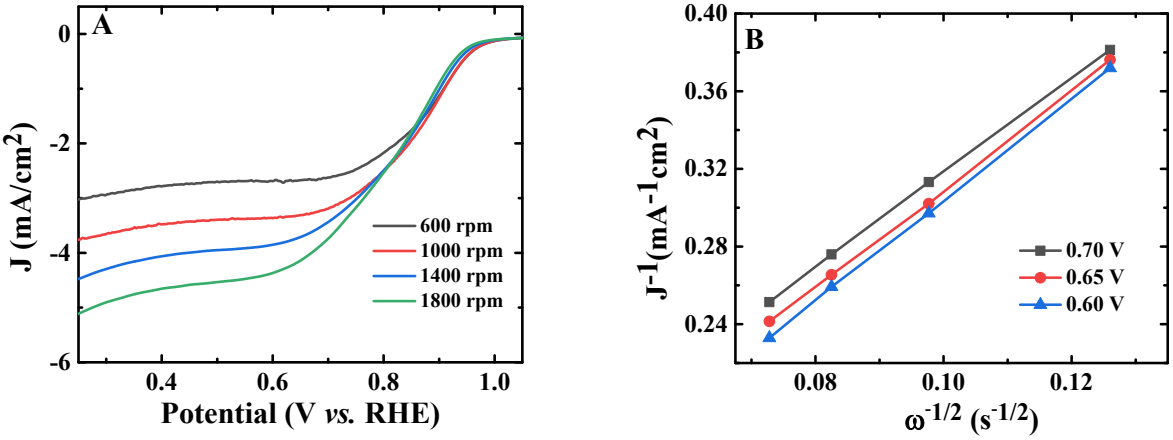

Fig. 13 (a and b) LSV curve at different rotation speed at 10 mV/s scan rate and the corresponding K-L plot for Pd/C, respectively

ESI-14

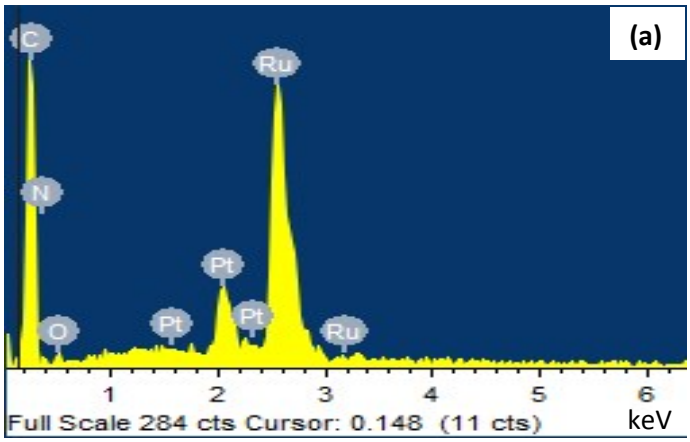

Element	Weight%	Atomic%
C K	38.27	68.22
N K	10.99	16.81
O K	4.55	6.09
Ru L	37.30	7.90
Pt M	8.89	0.98
Totals	100.00	

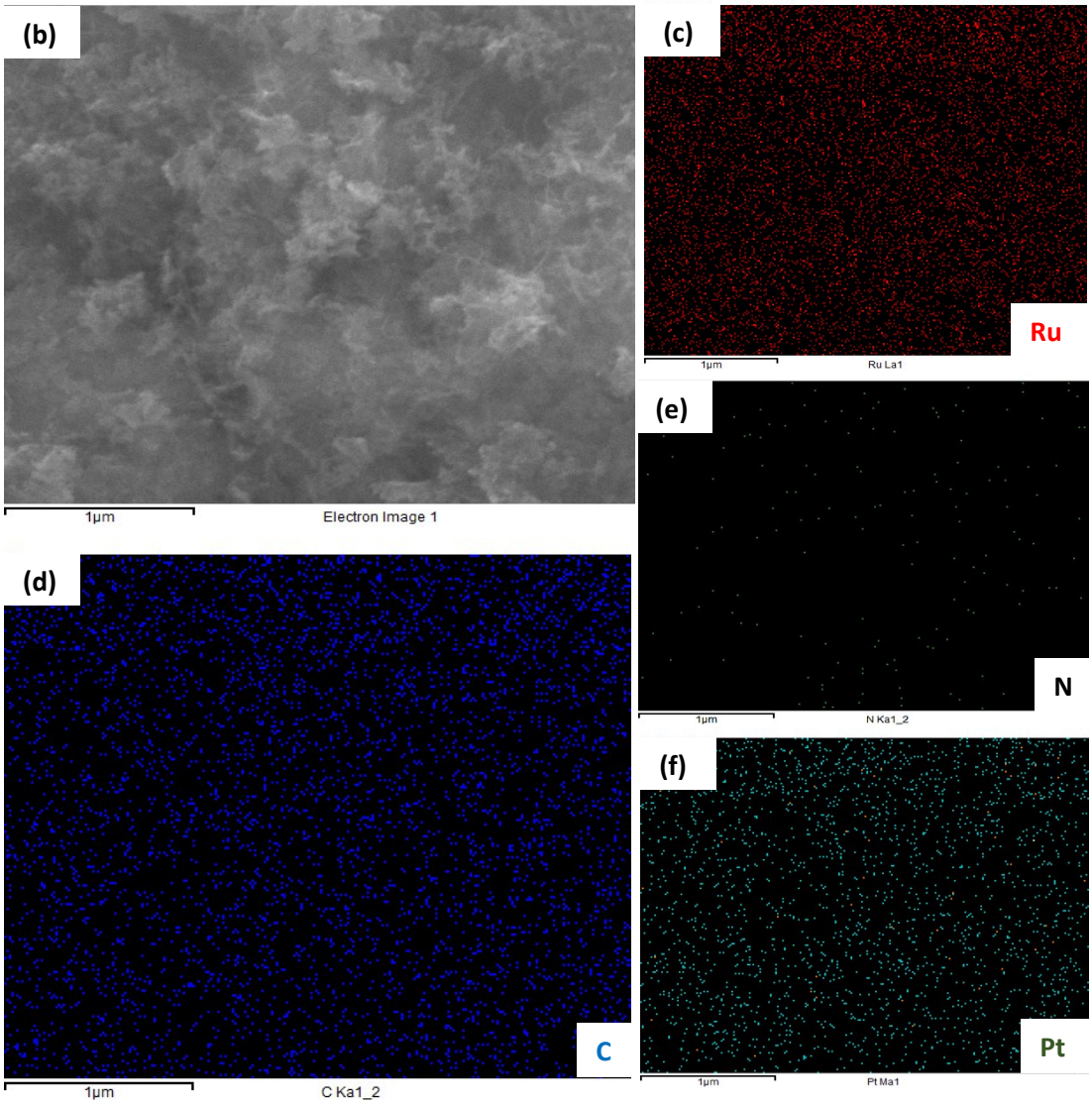

Fig. 14 (a) EDS spectra and the elemental composition table. (b) SEM image. (c-f) elemental mapping of C, N and Ru and Pd, respectively of Pt-Ru@NG

ESI-15

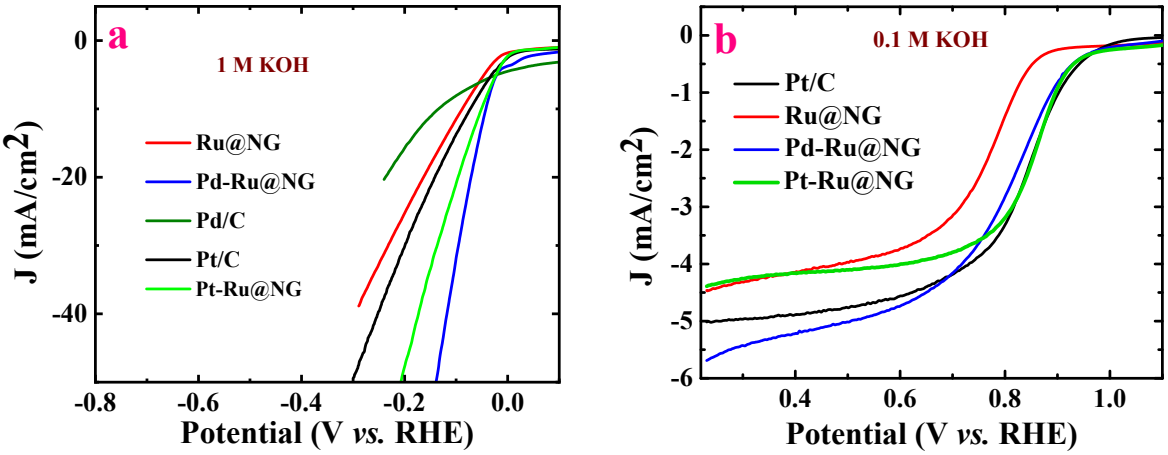

Fig. 15 (a and b) HER and ORR performance of Pt-Ru@NG hybrid catalyst compared to other as-synthesized catalysts in alkaline medium.

Table S-1: Comparison of HER performance of Ru or noble metal-based electrocatalyst other reported catalysts

Catalyst	Electrolyte	Potential (η) at 10 mA/cm^2 current density	Reference
Pd-Ru@rGO	**1 M KOH**	**42 mV**	**This work**
Pd-Ru@rGO	**1 M KOH**	**28 mV (iR corrected)**	**This work**
Pd-Ru@rGO	**1 M H_2SO_4**	**39 mV**	**This work**
Ru/C_3N_4/C	0.1 M KOH	79 mV	J. Am. Chem. Soc. 2016, 138, 16174-16181
PtCoFe@CN	1 M H_2SO_4	45 mV	ACS Appl. Mat. Interfaces 2017, 9, 3596.
Ru@C_2N	1 M KOH	17 mV	Nat. Nanotechnol. 2017, **12,** 441
$Pt_{13}Cu_{73}Ni_4$/CNF @CF	1 M H_2SO_4	70 mV (10 mA/cm^2)	ACS Appl. Mat. Interfaces 2016, 8, 3464
Ultrafine Ru/N-graphene	1 KOH	44 mV	Sustainable Energy Fuels 2017, **1**, 1028-1033
Ultrafine Ru/N-graphene	1 M H_2SO_4	74 mV	Sustainable Energy Fuels 2017, **1**, 1028-1033
RuP_2@N, P doped C	1 M KOH	52 mV	Angew. Chem. Int. Ed 2017, 56, 11559–11564
$Ni_{43}Ru_{57}$ nanoalloy	0.5 M H_2SO_4	41 mV	ACS Appl. Mat. Interfaces 2017, 9, 17326
Ru@NC	1 M KOH	32 mV	Energy Environ. Sci. 2018,11, 800-806
Ru-MoO_2	1 M KOH	29 mV	J. Mater. Chem. A. 2017, 5, 5475
Pt ML/Ag NF/NF	0.5 M H_2SO_4	70 mV	Sci. Adv. 2015, 1, e1400268
Cu_{2-x}S@Ru	1 M KOH	82 mV	Small 2017, 13, 1700052
PdCu@Pd NCs	0.5 M H_2SO_4	65 mV	ACS Appl. Mat. Interfaces 2017, 9, 8151

Pd@PdPt	0.5 M H_2SO_4	39 mV	J. Mater. Chem. A. 2016, 4, 16690.
Ru/NC	1 M KOH	21 mV	J. Mater. Chem. A, 2017,5, 25314-25318
Pt-Ru-Mo	Seawater	196 mV	J. Mater. Chem. A. 2016, 4, 6513
OsP_2@NPC	1 M KOH	90 mV	Chem. Commun., 2019, 55, 4399-4402
PdP_2@CB	1 M KOH	35.4 mV	Angew. Chem. Int. Ed., 2018, 57, 14862.
PdP_2@CB	0.5 M H_2SO_4	27.4 mV	Angew. Chem. Int. Ed., 2018, 57, 14862.

Table S-2 Comparison of ORR catalytic activity with other noble metals (bimetallic-) reported previously

Catalyst	Electrolyte	E_{onset} (V *vs* RHE)	$E_{1/2}$ (V *vs* RHE)	Reference
Pd-Ru@NG	**0.1 M KOH**	**1**	**0.8**	**This work**
$Au_{67}Pd_{33}$/CNs	0.1 M KOH	0.94	0.83	Catalysts 2018, 8, 65
Pd NPAs	0.1 M KOH	0.926	0.837	Eur. J. Inorg. Chem. 2017, 3, 535-539
7.5Pd–2.5Zn (300)	0.1 M $HClO_4$	0.85	-	J Appl Electrochem 2018, 48, 675
Pt_2Pd_1/C	0.1 M $HClO_4$	-	0.89	ACS Sustainable Chem. Eng. 2019, 7, 8419−8428
Mem2-PtAu/C	0.5 M H_2SO_4	0.843	-	J. Phys. Chem. C, 111, 7, 2007
Ni@Pd3/C NPs	0.1 M KOH	0.98 V	0.86	J. Mater. Chem. A, 2017,5, 9233-9240
Pd–Ni/C	0.1 M KOH	~0.97	~0.88	Int. J. Hydrogen Energy, 2016, 41, 22538 -22546
PdNi/CB (1:2)	0.1 M KOH	~0.98	~0.8	Electrochem. Commun., 2009, **11**, 1162 -1165
AgAu nanoparticles	0.1 M NaOH	0.917	-	Catal. Sci. Technol., 2016,6, 3317-3340